CENTRAL PIT CRATERS ACROSS THE SOLAR SYSTEM. N. G. Barlow[1], A. Maine[1], and S. Ferguson[1]
[1]Department of Physics and Astronomy, Northern Arizona University, Flagstaff, AZ 86011-6010 USA. Nadine.Barlow@nau.edu; am2935@nau.edu; snf38@nau.edu.

Introduction: Central pit (CP) craters display a central depression, either directly on the crater floor ("floor pit") or atop a central peak or rise ("summit pit"). These craters have now been reported on Mercury, Moon, Mars, Europa, Ganymede, Callisto, Dione, Rhea, and Tethys, and occassionally have been suggested to occur on Earth. Figure 1 shows examples of CP craters formed in crusts with low, intermediate, and high concentrations of volatiles (Mercury, Mars, and Ganymede, respectively).

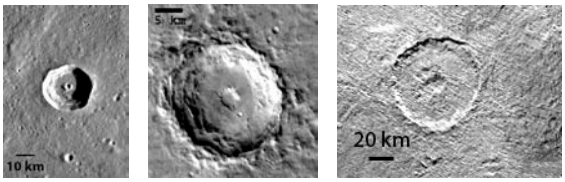

Figure 1: Example central pit craters on Mercury (left; 16.6-km-diameter, 19.99°N 63.62°E), Mars (middle; 20.7-km-diameter, 22.46°N 340.41°E), and Ganymede (right; 75.3-km-diameter, 67.3°S 158.9°E)

Central pit craters are more abundant on bodies with volatiles in their crusts, which led to early speculation that target volatiles were necessary for pit formation. Several formation models were proposed based on studies of CP craters on Ganymede, Callisto, and Mars: (1) Collapse of a central peak [1], (2) vaporization of target volatiles, either during crater formation [2] or during the modification stage [3], (3) melting of target volatiles with subsequent removal by drainage through subsurface fractures [4], and (4) collapse of a weaker subsurface layer [5]. Although CP craters were known on the Moon [6] and Mercury [7] in the 1970's, it is only recently with the availability of higher resolution images that CP craters on these volatile-poor bodies have been investigated in detail [8, 9]. The present study is the first to conduct a comprehensive comparative study of CP craters throughout the solar system in order to determine if a single formation model can explain all CP crater examples.

Methodology: We are utilizing the MESSENGER MDIS global mosaic (250 m/pixel), LRO WAC global mosaic (100 m/pixel), and THEMIS daytime IR global mosaic (100 m/pixel) to search for CP craters on Mercury, the Moon, and Mars, respectively. CP craters on Europa, Ganymede, and Callisto are identified using global mosaics composed of Galileo and Voyager images (60 km/pixel to 400 m/pixel resolutions). CP craters on Dione, Rhea, and Tethys are obtained from Cassini and Voyager image data with resolutions of 250-400 m/pixel.

CP craters are subdivided into floor pit or summit pit depending on visual and (when available) topographic information. Floor pits are further subdivided into those having an upraised rim partially or completely around the pit ("rimmed pit") and those without a pit rim ("unrimmed pit"). Global mosaic resolutions are not always sufficient to distinguish between pit types, so we utilize higher resolution images when available to help classify the central pit.

The geographic coordinates, diameter, preservational state, and underlying geologic unit of each CP crater are determined. Pit diameter also is measured and the ratio of pit diameter to crater diameter (D_p/D_c) is calculated. Detailed geomorphic and structural mapping of selected fresh CP craters on Mars is being conducted using the variety of image, mineralogic, and topographic datasets [10].

Observations—Pit Types: Table 1 summarizes the current results of our comparative study. In general we see a trend towards more summit pits and rimmed floor pits on volatile-poor bodies and more floor pit craters on bodies with higher concentrations of crustal volatiles. However, the overall number of CP craters is much lower on volatile-poorer bodies (Mercury and the Moon). Xiao et al. [8] reported many more CP craters on the Moon than we found in this analysis—many of their central pits appear to be natural depressions in central peak complexes and floor deposits.

Observations—D_p/D_c: Table 1 shows that D_p/D_c tends to be higher for floor pit craters, indicating that floor pits are larger relative to their parent crater than summit pits. D_p/D_c of floor pits is consistently higher for bodies with volatile-rich crusts (Ganymede, Tethys, Dione, and Rhea) than for the volatile-poorer bodies (Mercury and the Moon), with the ice-rock mixed crust of Mars (estimated at ~20% ice by volume) lying between the values for the volatile-richer and volatile-poorer bodies.

We see no strong trend in D_p/D_c as a function of gravity for pits on the volatile-rich worlds of Ganymede, Rhea, Dione, and Tethys. For Mars, Mercury, and the Moon, we do see a trend toward larger D_p/D_c as gravity increases for both floor pits and summit pits.

Observations—Morphology: All CP craters identified to date on Mercury are either summit pit or rimmed floor pit craters. Of the 10 lunar CP craters, two are summit pit and seven are rimmed floor pits. The percentage of floor pit craters increases for bodies

with volatile-richer crusts. There is some debate as to whether summit pit craters actually exist on Ganymede [11] or if all pit craters are floor pits with many occurring on updomed floors. Both rimmed and unrimmed floor pits are seen on Mars and Ganymede.

Detailed geomorphic and structural mapping of the 16.3-km-diameter rimmed floor pit crater Esira on Mars (8.9°N 313.4°E) reveals uplifted megablocks in the pit rim [10]. In addition, impact melt appears to have flowed from the crater floor into the pit.

Observations—Pit Depth: Craters display a well-established depth-diameter (d/D) relationship [12] and the question arises whether central pits show a similar d/D relationship. We have used shadow length measurements to determine the depths of a sample of Martian floor pits and have investigated the results as a function of crater preservational state (Fig. 2). The ratio of pit depth to pit diameter (d_p/D_p) is random even for fresher craters (preservational states of 5-7), indicating that there is unlikely to be a standard d/D relationship for pits as there are for craters.

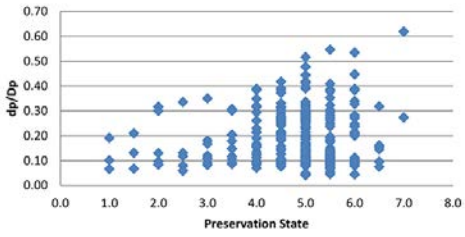

Figure 2: Pit depth to diameter ratio (dp/Dp) as a function of crater preservational state (0.0 = "ghost crater"; 7.0 = pristine crater).

Discussion: Although this study is still in its early stages, we have identified some trends that provide insight into pit formation processes. Floor pits tend to be larger relative to their parent crater than summit pits and the former also are more prevalent as crustal volatile content increases. Although D_p/D_c tends towards larger values as surface gravity increases from the Moon to Mercury to Mars for both floor and summit pits, a similar trend is not seen among the bodies with volatile-rich crusts (Tethys, Dione, Rhea, and Ganymede). This suggests that collapse of a weaker material may be responsible for pit formation on volatile-poorer bodies but that crustal volatiles can mask and/or enhance this effect. The prevalence of rimmed floor pits on all bodies and the identification of uplifted megablocks in Esira's pit rim indicate that uplift is involved in pit formation followed by collapse. However, the presence of central peak craters in the same regions and diameter ranges as CP craters indicates that peak collapse in weaker target materials is not the entire story. Identification of impact melt flowing from Esira's floor into its central pit constrains the pit formation to being essentially contemporaneous with crater formation. At this stage of the study, the data indicate that central pit formation models involving only collapse and/or only volatile targets can be eliminated from consideration.

Acknowledgements: This work is supported by NASA MDAP award NNX12AJ31G and NASA PGG award NNX14AN27G.

References: [1] Passey Q.R. and Shoemaker E.M (1982) *Satellites of Jupiter*, UAz Press, 379-434. [2] Wood C.A. et al. (1978) *Proc. 9th LPSC*, 3691-3709. [3] Williams N.R. et al. (2015) *Icarus, 252*, 175-185. [4] Senft L.E. and Stewart S.T. (2011) *Icarus, 214*, 67-81. [5] Greeley R. et al. (1982) *Satellites of Jupiter*, UAz Press, 340-378. [6] Allen C.C. (1975) *The Moon, 12*, 463-474. [7] Schultz P.H. (1988) *Mercury*, UAz Press, 274-335. [8] Xiao Z. and Komatsu G. (2013) *Planet. Space Sci., 82-83*, 62-78. [9] Xiao Z. et al. (2014) *Icarus, 227*, 195-201. [10] Maine A. et al. (2015) *46th LPSC*, abstract #2944. [11] Bray V.J. et al. (2012) *Icarus, 217*, 115-129. [12] Melosh H. J. (1989) *Impact Cratering: A Geologic Process*, Oxford Univ. Press, 245 pp.

Table 1: Morphometric Comparison of Central Pit Craters

	Mercury	Moon	Mars	Ganymede	Tethys*	Dione*	Rhea*
Number floor pits	7	8	1161	471	13	12	12
Number summit pits	15	2	625	0			
D_c range (km) floor	13.9-30.7	10.5-55.4	5.0-114.0	12.0-143.8	10.9-450.0	17.0-74.9	16.7-230.0
D_c range (km) summit	16.2-30.7	28.9-30.4	5.1-125.4	NA			
Median D_c (km) floor	17.2	35.3	13.8	38.1	22.5	32.9	46.1
Median D_c (km) summit	25.0	29.7	14.4	NA			
D_p/D_c range floor	0.08-0.15	0.08-0.16	0.02-0.48	0.06-0.43	0.14-0.42	0.15-0.32	0.17-0.33
D_p/D_c range summit	0.07-0.15	0.06-0.11	0.02-0.29	NA			
Median D_p/D_c floor	0.14	0.12	0.16	0.20	0.18	0.22	0.23
Median D_p/D_c summit	0.11	0.08	0.12	NA			
Surface gravity (m/s^2)	3.7	1.62	3.71	1.43	0.15	0.23	0.26

* Pits have not yet been divided into floor and summit pits.